Journal of Materials Chemistry A

Accepted Manuscript

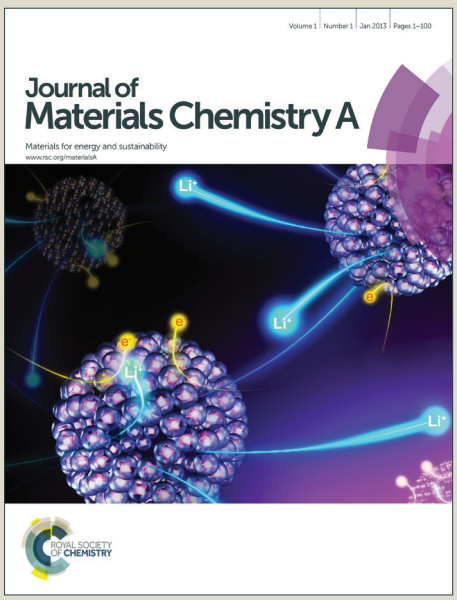

ROYAL SOCIETY OF CHEMISTRY

www.rsc.org/materialsA

Journal Name

RSCPublishing

COMMUNICATION

Molybdenum carbide nanocrystals embedded N-doped carbon nanotubes as electrocatalysts for hydrogen generation

Cite this: DOI: 10.1039/x0xx00000x

Received 00th January 2012,
Accepted 00th January 2012

DOI: 10.1039/x0xx00000x

www.rsc.org/

Kai Zhang, Yang Zhao, Diyu Fu and Yujin Chen*

Molybdenum carbide nanocrystals with a size less than 3 nm embedded N-doped carbon nanotubes were fabricated. Due to small size, tubular characteristic and high conductivity, the hybrid nanotubes exhibit superior activity for hydrogen evolution reaction, including small overpotential, large cathodic current density and high exchange current density.

Hydrogen, as a green fuel with high gravimetric energy density, is a promising candidate for traditional petroleum fuels in the future. Electrochemical water splitting is one of efficient ways to produce hydrogen.[1] To achieve efficient water splitting for a wide range of applications, active catalysts for the hydrogen evolution reaction (HER) are requried.[1] Some precious metals, such as platinum, have high efficiency in the HER, however, their high cost and scarcity limit their large scale applications. Therefore, much attention has been paid to search for and develop non-precious catalysts. Recently, molybdenum-based materials, such as molybdenum disulfide (MoS_2),[2] molybdenum carbide (Mo_2C),[3 –10] molybdenum phosphide (MoP),[11] and molybdenum nitride (MoN),[12] have been exploited as electrocatalysts for HER in acidic media. Among these molybdenum-based materials, Mo_2C exhibited remarkable HER activities in both acidic and basic conditions due to its similar electronic structures to that of noble metals.[3 –10] Recent results showed that crystal phase, surface area, morphology, and conductivity had very important effects on the catalytic performance of molybdenum carbide-based materials towards HER. Wan *et al* synthesized different phases of molybdenum carbide (α, β, γ, η-phases) and investigated their HER activities.[5] Their results revealed that γ-MoC exhibited the second highest HER activity among all four phases of molybdenum carbide, but superior stability in an acidic solution.[5] Nanoporous molybdenum carbide nanowires exhibited excellent HER activity with a low onset overpotential of about 70 mV vs. RHE.[6] Chen *et al* prepared β-Mo_2C nanoparticles by *in situ* carburization of ammonium molybdate on carbon nanotubes (CNTs) and XC-72R carbon black.[7] The CNT-supported and carbon black-supported Mo_2C showed superior electrocatalytic activity and stability towards the HER compared to the bulk Mo_2C.[7] In terms of the X-ray absorption analysis results, they attributed the enhancement of the HER activity of the hybrids to the electronic modification, i.e., the anchored configuration induces a charge-transfer from molybdenum to carbon, which further downshifts the d-band center of molybdenum, and thereby decreases its hydrogen binding energy (relatively moderate Mo–H bond strength).[7] Such electronic modification was also found by Youn *et al* in the Mo_2C nanoparticles on CNT-graphene hybrid support by the same analytical technique.[9] At the same time, these carbon-supported Mo_2C materials obtained through *in situ* carburization at a high temperature possess higher conductivities than that of pure Mo_2C, which is suitable for fast electron transfer. Therefore, robust conjugation with conductive supports is a very efficient strategy to improve the HER activitie of Mo_2C materials.

The carbon supporting materials, such as carbon black, CNTs and graphene etc., are almost inert for HER, which may suppress the gravimetric current density of Mo_2C-based electrocatalysts. Recently, both density functional theory (DFT) calculations and experimental results proved that N dopant could downshift the valence bands of active carbons in graphene, resulted in enhanced reactivity of N-doped graphene toward HER compared to graphene without heteroatom doping.[13] Zou *et al* reported excellent activity of cobalt-

embedded N-rich carbon nanotubes toward HER due to N doping and concomitant structural defects. [14]

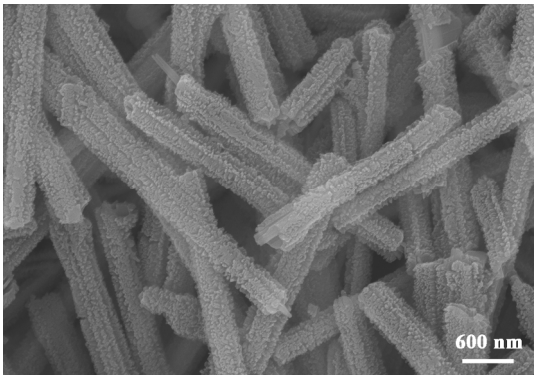

Fig. 1 SEM images of MoO_3/PANI hybrids

Herein, we describe a strategy based on *in situ* solid reaction to fabricate Mo_2C embedded in N-doped carbon nanotubes (NCNTs), which can serve as highly active electrocatalyst for HER under acidic, neutral or basic media. Despite recent studies on the electrocatalytic activities of carbonaceous material-supported Mo_2C nanostructures,[7–10] it is the first time Mo_2C embedded N-doped CNTs (Mo_2C-NCNTs) are reported to catalyze HER. The synthesized Mo_2C-NCNTs as HER catalyst offers the following advantages: (i) The Mo_2C-NCNTs are prepared by a simple and environmentally friendly carburization process, i.e., pyrolyzing precursor MoO_3/polyaniline (MoO_3/PANI) hybrids under an inert atmosphere. During the whole synthetic procedure, no toxic and dangerous reactant gases such as CH_4, C_2H_6, and CO were used. The synthetic method presented here is similar to one based on the nanoscale Kirkendall effect,[15] which greatly facilitates the formation of tubular structures. Furthermore, the mean size of Mo_2C nanocrystals is less than 3 nm, which is much smaller than those of reported Mo_2C nanostructures. The features of small size, and tubular morphology of Mo_2C-NCNTs greatly favor in their contact with electrolyte efficiently, and thereby significantly accelerate their interfacial electrocatalytic reactions. (ii) N-dopants in the composite play a positive role in electrocatalytic activity of Mo_2C-NCNTs compared to other types of carbonaceous supports. On one hand, nitrogen atoms are more active than carbon atoms as reacted with protons or water; on the other hand, the electronegativity of nitrogen is higher than that of carbon, making carbon atoms adjacent to N dopants become catalytic active sites.[14] Thus, NCNTs are more active for the HER than other carbon supports such as CNTs and graphene sheets. Consequently, the NCNT support does not suppress the gravimetric current density of the composite catalysts significantly. (iii) NCNT in the composite can significantly improve the whole conductivity of the electrocatalyst, and thus increases charge transfer rate during the HER process. As a result, Mo_2C-NCNTs exhibited excellent HER activity with low overpotentials of 72 and 147 mV vs RHE for driving cathodic current densities of 1 and 10 mA cm^{-2} in acidic media, respectively. Furthermore, the hybrid nanotubes also exhibit high activity and long-term stability in basic and neutral solutions. Compared to most of other Mo_2C nanostructures reported so far, the Mo_2C-NCNTs show superior HER activity.

MoO_3/PANI hybrids were first fabricated by our previous method with a modification.[16] The detailed synthesis processes are also described in the Electronic Supplementary Information (ESI).† A typical SEM image (Fig. 1) clearly shows that MoO_3/PANI hybrids were synthesized in high yields with lengths and diameters of about several micrometers and 400 nm, respectively.† After the hybrids were annealed at 700°C for 3 h under an Ar flow, interesting tube-like nanostructures were obtained. In the X-ray diffraction (XRD) (Fig. S1), the peaks labeled by Miller indices can be indexed to crystalline Mo_2C (JCPDs PDF no. 35-0787).† In addition, peaks coming from monoclinic MoO_2 (JCPDs PDF no.86-0135) are also found. The densities of the diffraction peaks are great lower than those of Mo_2C, which implies that small amount of MoO_2 presented in the final product.

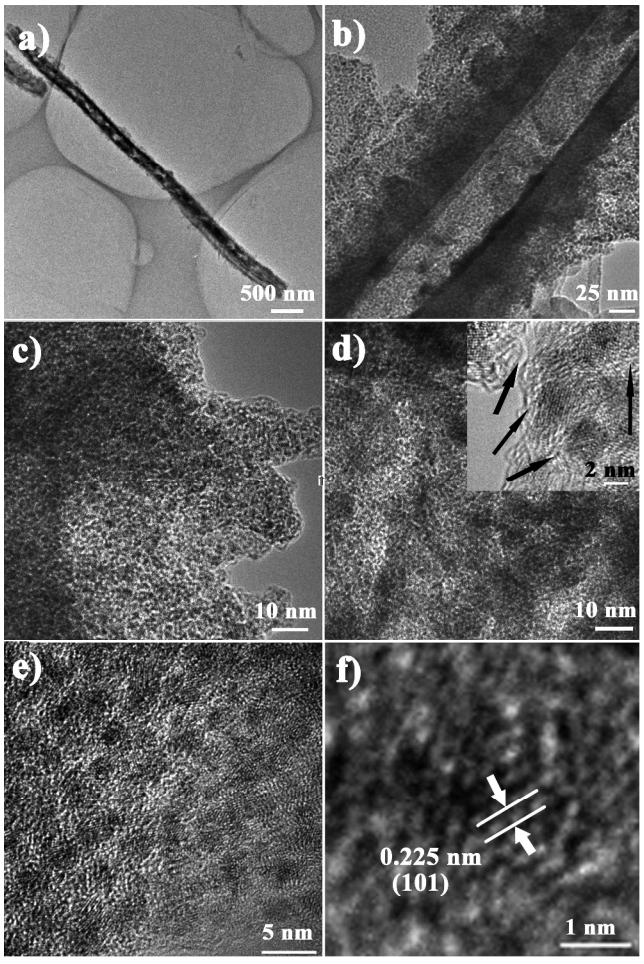

Fig. 2 a) Low magnification, b-e) high-magnification TEM and f) HRTEM images of Mo_2C-NCNTs, and the inset in d) showing amorphous carbon layers.

Structural details of the Mo_2C-NCNTs were further analyzed by scanning electron microscopy (SEM) and transmission electron microscopy (TEM). SEM image (Fig. S2) shows that

Mo_2C-NCNTs have lengths and diameters of about several micrometers and 250 nm, respectively.† The inset in the image shows that the ends of the Mo_2C-NCNTs are open. TEM images (Fig. 2(a) and Fig. 2(b)) clearly demonstrate that the final product exhibits tubular characteristic with a thickness of the walls in the range of 50– 140 nm. Fig. 2(c) and (d) show the magnification TEM images in the external and inner regions, respectively. It can be found that small Mo_2C particles are dispersed well in the both regions. High-resolution TEM (HRTEM) image indicates that the mean size of these Mo_2C particles is less than 3 nm, as shown in Fig. 2(e). The small Mo_2C nanoparticles are embeded in amorphous carbon layers, as indicated by the arrows in the inset of Fig. 2(d). The lattice spacing value labeled in Fig. 2(f) is about 0.225 nm, corresponding to (101) crystal plane of Mo_2C. Notably, to the best of our knowledge, Mo_2C prepared in the present work possesses the smallest size among previously reported Mo_2C nanostructures so far.[3–10, 17] For example, the sizes of Mo_2C nanoparticles in Mo_2C nanowires,[6] loaded on the CNT-graphene hybrid support,[9] embeded in graphitic carbon sheets,[8] stabled on graphene sheets,[10] and supported on CNTs[7] are 10 – 15, 8.5, 5 –23, 10, and 7–15 nm, respectively.

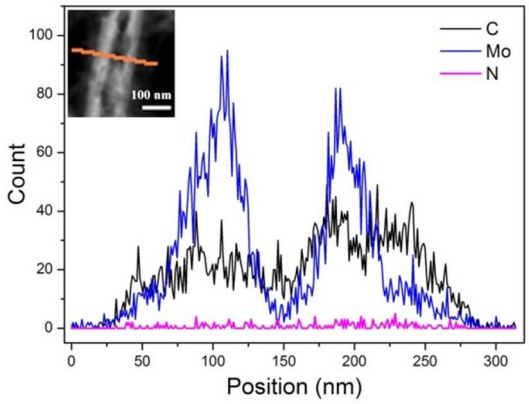

Fig. 3 EDX elemental scanning mappings of Mo_2C-NCNTs, and the inset showing the corresponding STEM image.

An annular dark-field (ADF) scanning transmission electron microscopy (STEM) image and the corresponding energy dispersive X-ray spectrometry (EDX) elemental scanning mappings were conducted to determine the composition distribution of the Mo_2C-NCNTs, as shown in Fig. 3. It can be clearly found that the C, Mo and N elements are uniformly distributed in the walls of the NCNTs. In addition, this result also confirms the tubular characteristic of the Mo_2C-NCNTs. X-ray photoelectron spectroscopy (XPS) further confirms the presence of N element in the NCNTs (Fig. S3(a)).† Fig. S3(b) shows the high-resolution XPS spectrum of N 1s, in which the peaks at 398.4 and 401.2 eV can be assigned to pyridinic and quaternary N species, respectively.† The percentage of N species in the Mo_2C-NCNTs is calculated to be 7.03 at%. The peaks at binding energy of 228.5 and 231.6 eV in the high resolution of Mo 3d XPS spectrum (Fig. S3(c)) can be assigned to $3d_{5/2}$ and $3d_{3/2}$ of $Mo^{(II)}$, respectively.[2c, 18] Other peaks at the binding energies of 229.2 and 232.3 eV for $Mo^{(IV)}$ coming from MoO_2, and 232.4 and 235.5 eV for $Mo^{(VI)}$ due to surface oxidation of Mo_2C are also observed (Fig. S3(c)).[2c, 18] Fig. S3(d) shows high-resolution C 1s XPS spectrum, in which the asymmetric peak indicates that C–O (at 286.0 eV) and C=N (at 287.0 eV) groups exist in the layers of the Mo_2C-NCNTs.

Nitrogen adsorption and desorption isotherms of shows that the Mo_2C-NCNTs have a Brunauer−Emmet−Teller (BET) surface area of 27.6 m^2 g^{-1}.† The average pore diameter is 19.7 nm (Fig. S4(b)), calculated from the desorption branch of the nitrogen isotherm obtaining using the Barret–Joyner–Halenda (BJH) method, and the corresponding BJH desorption cumulative volume is 0.16 cm^3 g^{-1}.† Such porous characteristic and large pore volume allow the inner active sites of the Mo_2C-NCNTs can be fully contacted with electrolyte, and further make the electrolyte diffusion in/outward electrode materials easily, which is favor of the improvement of the electrochemical catalytic activity of the Mo_2C-NCNTs.

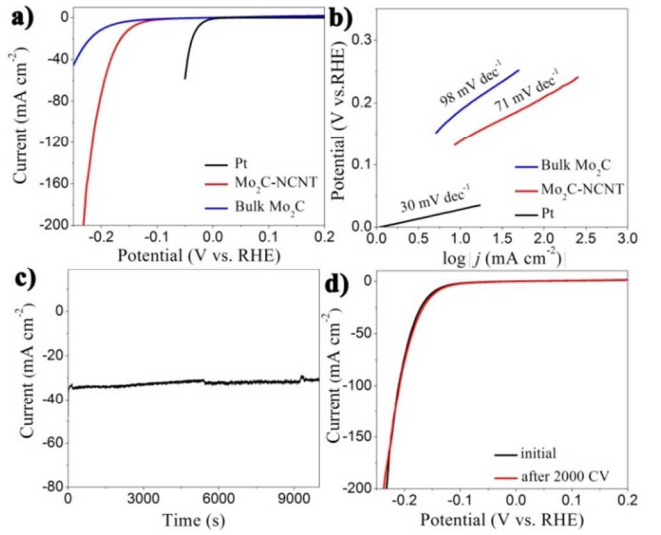

Fig. 4 a) Polarization curves and b) Tafel plots of **Mo_2C-NCNTs, Pt, and bulk Mo_2C**, c) Cycling stability of Mo_2C-NCNTs at an overpotential of 180 mV, d) the polarization curves before and after potential sweeps for 2000 cycles **at an overpotential widow from 0.2 to -0.21 V** in 0.5 M H_2SO_4 solution .

Electrochemical measurements of the Mo_2C-NCNTs loaded on carbon paper were carried out in 0.5 M H_2SO_4 solution using a three-electrode setup to evaluate their HER activities.† For comparison, Pt, bulk Mo_2C, CNTs, graphene sheets and t-PANI were also measured. Fig. 4(a) shows the polarization curves with a sweep rate of 5 mV s^{-1}. Pt catalyst exhibits expected HER activity with a near zero overpotential (η), whereas bulk Mo_2C exhibits poor HER activity. In contrast, the Mo_2C-NCNTs exhibit a small onset overpotential of 72 mV, which is much smaller than that of bulk Mo_2C (83 mV). Furthermore, for driving cathodic current densities of 1 and 10 mA cm^{-2}, the Mo_2C-NCNTs only need overpotentials of 72 and 147 mV, respectively. The cathodic current densities (J) of the Mo_2C-NCNTs are comparable to the values of graphene and CNT-supported Mo_2C nanoparticles, [6, 7, 10] and greatly larger than those of other Mo_2C-based nanostructures. [5, 8, 17] Furthermore,

the cathodic current density can be up to 72.7 mA cm^{-2}at η= 200 mV, which is the largest value among the reported Mo_2C catalysts (Table S1) †. This indicates superior catalytic activity of the Mo_2C-NCNTs for HER. The large current density at a low overpotential means prominent hydrogen evolution behavior, evidenced by the continuous and small bubbles escaped from the Mo_2C-NCNT electrode surfaces (video, ESI).†

For further study of HER activity of the Mo_2C-NCNTs, Tafel plots were fitted to Tafel equation ($\eta = a + b\log|j|$), where b is the Tafel slope. As shown in Fig. 4(b), the Pt catalyst exhibits a Tafel slope of 30 mV dec^{-1}, which is consistent with the reported values. The Tafel slope of the the Mo_2C-NCNTs is 71 mV dec^{-1}, much lower than that of the bulk Mo_2C (98 mV dec^{-1}), suggesting both electrocatalysts may proceed a Volmer-Heyrovsky mechanism, in which Volmer reaction is the rate-limiting step. [4, 19] Recent researches have demonstrated that the Tafel slopes can be obtained by electrochemical impedance spectroscopy (EIS) analysis, which can effectively eliminate the effect of some additional factors, such as different choice of overpotential regions and different ways for iR-corrections, on the HER mechanism.[6, 7] Fig. S6 shows Nyquist plots of the Mo_2C-NCNTs at different overpotentials. † As fitted from the experimental data, a two time-constant model can be used to describe the HER behavior on the Mo_2C-NCNT electrode surfaces (the inset in Fig. S5).† In the equivalent circuit, R_s is the series resistance, R_{ct} denotes the charge transfer resistance dependent on the overpotential, R_p is related to the porosity of the electrode surface, and C_1 and C_2 represents the double layer capacitance.[6, 7]. For comparison, the Nyqusit plots and the equivalent circuit model for bulk Mo_2C are also conducted, as shown in Fig. S6.† According to the Nyquist plots and the corresponding equivalent circuit models, the values of R_{ct} at different overpotentials can be easily extracted. Plots of overpotential *verves* log R_{ct}^{-1} (Fig. S7) show that the Tafel slope is 77 mV dec^{-1} for the Mo_2C-NCNTs, and 102 mV dec^{-1} for bulk Mo_2C.† The values are very close to those obtained based on Tafel equation, confirming that the hydrogen evolution catalyzed by the Mo_2C-NCNTs and bulk Mo_2C occurs via a Volmer-Heyrovsky mechanism. The Tafel slope of the Mo_2C-NCNTs is smaller than that of bulk Mo_2C, suggesting much faster proton discharge kinetics on the Mo_2C-NCNT electrode than that on the bulk Mo_2C electrode.

Exchange current density (j_0) is another important parameter to evaluate electrochemical performance of electrocatalysts, which represent the intrinsic activities of electrocatalysts for HER. As shown in Table S1, the exchange current density determined by Tafel equation for the Mo_2C-NCNTs is 114.6 μA cm^{-2}, which is higher than those of the previously reported Mo_2C-based nanostructures. The Mo_2C-NCNTs exhibit the highest exchange current density (Table S1), which may attributed to more active sites of Mo_2C nanocrystals induced by their very smaller size (less than 3 nm) and tubular and porous characteristics.[7]†

The superior HER activities of the Mo_2C-NCNTs, including small onset overpotential, large cathodic current density, and high exchange current density, can be attributed to their lower charge transfer resistances and higher interfacial capacitances.[6, 7] Table S2 shows the comparison of the charge transfer resistances and interfacial capacitances between the Mo_2C-NCNTs and the bulk Mo_2C at different overpotentials.† At applied overpotentials, the all charge transfer resistances of the Mo_2C-NCNTs are great lower than those of the bulk Mo_2C; whereas the interfacial capacitances of the former are significantly higher than those of the latter. This suggests that the Mo_2C-NCNTs not only exhibit much faster charge transfer kinetics, but also have much larger contact area between the catalysts and electrolyte than the bulk Mo_2C. These advantages of the Mo_2C-NCNTs as electrocatalysts for HER may be related to the following factors. (i) Mo_2C nanocrystals with a mean size less than 3 nm result in more abundant active sites for HER. (ii) NCNT in the composite can significantly improve the whole conductivity of the electrocatalyst (Table S2), and thus increases charge transfer rate during the HER process. † (iii) The porous and tubular characteristics of the Mo_2C-NCNTs allow more active sites for HER to contact with electrolyte, which is helpful to the improvement of the overall efficiency of HER. (iv) Compared to other carbon supports such as CNTs and graphene, the N-doped carbon materials (NCNT) in the composite would not suppress the HER activity at least because N-doped graphene and cobalt-embedded N-rich CNTs showed enhanced HER activities.[13, 14] An indirect evidence for the conclusion is in that t-PANI nanorods exhibit slightly better activities for HER in acidic media than the commercial CNTs and graphene sheets, as shown in Fig. S8. † To further clarify the important role of N-dopants in the HER activity in the composite, we prepared CNTs supported Mo_2C nanoparticles (Mo_2C-CNTs) and compared their HER activity with those of Mo_2C-NCNTs. The Mo_2C-CNTs were synthesized by a previously reported method with a modification.[7] The diffraction peaks from both CNTs and Mo_2C can be found in the XRD pattern of Mo_2C-CNTs (Fig. S9).† It suggests that the composite consists of Mo_2C and CNTs, similar to the previous results.[7] TEM image shows that Mo_2C nanoparticles with a size of 5 –20 nm are coated on the CNTs (Fig. S10(a)).† The lattice spacing values labeled in HRTEM image (Fig. S10(b)) are 0.236 and 0.335 nm, corresponding to (002) planes of Mo_2C and CNTs, respectively.† Fig. S11 compares the HER performance between Mo_2C-CNTs and Mo_2C-NCNTs in 0.5 M H_2SO_4 solution.† For driving cathodic current density of 10 mA cm^{-2}, Mo_2C-CNTs needs an overpotential of 179 mV, great higher than that of Mo_2C-NCNTs (147 mV). Although Tafel slope of Mo_2C-NCNTs (71 mV dec^{-1}) is slightly higher than that of Mo_2C-CNTs (65 mV dec^{-1}), the exchange current density of the former is about 5.8 times larger than that of the latter. In addition, EIS measurements show that the R_{ct} values of Mo_2C-NCNTs are comparable to those of Mo_2C-CNTs at 100–250 mV, suggesting that N-doped CNTs also have a good conductivity (Fig.S12 and Table S3).† The results above demonstrate that N-doped CNTs play a positive role in HER activity.

The long-term durability of the Mo_2C-NCNTs was examined by electrolysis at a given potential. As shown in Fig. 4(c), the cathodic current densities at overpotential of 180 mV have no significant degradation over 10 000 s. The stability of the Mo_2C-NCNTs in acidic media was also investigated by sweeping the catalysts for 2000 cycles. After the cycles, the negligible current loss is observed, as shown in Fig. 4(d)**.** These results indicate that the Mo_2C-NCNTs exhibit excellent electrochemical stability in acidic electrolyte. In addition, the Mo_2C-NCNTs exhibit good activity and stability for HER in basic and neutral solutions. For driving cathodic current densities of 10 mA cm^{-2}, the Mo_2C-NCNTs in 1 M KOH (pH =14) and in phosphate buffer (pH =7) need overpotentials of 257 and 645 mV, respectively (Fig. S13(a) and Fig. S14(a)), which are significantly smaller than those of the bulk Mo_2C.† At the same time, electrolysis at given potentials can continuously occur without degradation in cathodic current densities as the Mo_2C-NCNTs applied as catalysts in the basic and neutral solutions, as shown in Fig. S13(b) and Fig. S14(b), respectively. †

Conclusions

Molybdenum carbide nanocrystals embedded N-doped carbon nanotubes were fabricated by an *in situ* solid reaction where no toxic and dangerous reactant gases were used. The synthetic method presented here is similar to one based on the nanoscale kirkendall effect, greatly facilitates the formation of tubular structures with a porous characteristic. TEM analysis reveals that Mo_2C nanocrystals embedded in the wall of the N-doped nanotubes have a mean size less than 3 nm, greatly smaller than those of previously reported Mo_2C nanostructures. Due to small size, tubular characteristic and high conductivity, the hybrid nanotubes exhibit superior activity for hydrogen evolution reaction. For driving cathodic current density of 10 mA cm^{-2}, only a low overpotential of 147 mV vs RHE is required as the hybrid nanotubes used as electrocatalysts for HER in acidic media. Furthermore, the hybrid nanotubes also exhibit high activity and long-term stability in basic and neutral solutions. The present strategy may open a way for the development of highly active non-precious catalysts for HER.

Acknowledgements

We thank the National Natural Science Foundation of China (Grant Nos. 51272050 and 21271053), the Innovation Foundation of Harbin City (2012RFXXG096), and also the 111 project (B13015) of Ministry Education of China to the Harbin Engineering University.

Notes and references

Key Laboratory of In-Fiber Integrated Optics, Ministry of Education, and College of Science, Harbin Engineering University, Harbin 150001, China. Fax: 86-451-82519754; Tel: 86-451-82519754; E-mail: chenyujin@hrbeu.edu.cn

Electronic Supplementary Information (ESI) available: [Experimental details, comparisons of HER performances among different Mo_2C catalysts, comparison of charge-transfer resistances between bulk Mo_2C and Mo_2C-NCNT at different overpotentials, XRD, SEM, XPS, Nitrogen adsorption and desorption isotherms, Nyquist plots of impedance spectroscopy, and the HER activity of Mo_2C-NCNTs, Nyquist plots of impedance spectroscopy analysis and the corresponding equivalent circuits of bulk Mo_2C, Mo_2C-CNTs and Mo_2C-NCNTs, plots of overpotential *verves* log R_{ct}^{-1} for Mo_2C-NCNTs and bulk Mo_2C, XRD and TEM of Mo_2C-CNTs, and Polarization curves and Tafel plots of Mo_2C-CNTs]. See DOI: 10.1039/c000000x/

1. a) M. G. Walter, E. L. Warren, J. R. McKone, S. W. Boettcher, Q. X. Mi, E. A. Santori and N. S. Lewis, *Chem. Rev.*, 2010, **110**, 6446 – 6473.; b) T. R. Cook, D. K. Dogutan, S. Y. Reece, Y. Surendranath, T. S. Teets and D. G. Nocera, *Chem. Rev.*, 2010, **110**, 6474 – 6502.; c) D. V. Esposito, S. T. Hunt, Y. C. Kimmel and J. G. Chen, *J. Am. Chem. Soc.*, 2012, **134**, 3025 – 3033.; d) N. S. Lewis and D. G. Nocera, *Proc. Natl. Acad. Sci. USA*, 2006, **103**, 15729 – 15735.
2. a) B. Himmemann, P. G. Moses, J. Bonde, K. P. Jørgensen, J. H. Nielsen, S. Horch, I. Chorkendorff and J. K. Nørskov, *J. Am. Chem. Soc.,* 2005, **127**, 5308-5309.; b)T. F. Jaramillo, K. P. Jørgensen, J. Bonde, J. H. Nielsen, S. Horch and Ib Chorkendorff, *Science*, 2007, **317**, 100-102.; c) H. Vrubel, D. Merki and X. Hu, *Energy Environ. Sci.*, 2012, **5**, 6136-6144; d) J. Kibsgaard, Z. Chen, B. N. Reinecke and T. F. Jaramillo, *Nat. Mater.,* 2012, **11**, 963-969; e) H. I. Karunadasa, E. Montalvo, Y. J. Sun, M. Majda, J. R. Long and C. J. Chang, *Science*, 2012, **335**, 698-702; f) J. F. Xie, H. Zhang, S. Li, R. X. Wang, X. Sun, M. Zhou, J. F. Zhou, X. W. Lou and Y. Xie, *Adv. Mater.,* 2013, **25**, 5807-5813; g) J. Xie, J. Zhang, S. Li, F. Grote, X. Zhang, H. Zhang, R. Wang, Y. Lei, B. Pan and Y. Xie, *J. Am. Chem. Soc.,* 2013, **135**, 17881-17888; h) S. Zhuo, Y. Xu, W. Zhao, J. Zhang and B. Zhang, *Angew. Chem. Int. Ed.,* 2013, **52**, 8602-8606; i) T. Wang, L. Liu, Z. Zhu, P. Papakonstantinou, J. Hu, H. Liu and M. Li, *Energy Environ. Sci.*, 2013, **6**, 625–633; j) K. Zhang, Y. Zhao, S. Zhang, H. Yu, Y. J. Chen, P. Gao and C. L. Zhu, *J. Mater. Chem. A*, 2014, **2**, 18715 – 18719.
3. H. Vrubel and X. Hu, *Angew. Chem. Int. Ed.*, 2012, 51, 12703 – 12706.
4. W. F. Chen, J. T. Muckerman and E. Fujita, *Chem. Commun.*, 2013, **49**, 8896 – 8809.
5. C. Wan, Y. N. Regmi and B. M. Leonard, *Angew. Chem. Int. Ed.*, 2014, **53**, 6407 – 6410.
6. L. Liao, S. Wang, J. Xiao, X. Bian, Y. Zhang, M. D. Scanlon, X. Hu, Y. Tang, B. Liu and H. H. Girault, *Energy Environ. Sci..*, 2014, **7**, 387 – 392.
7. W. F. Chen, C. H. Wang, K. Sasaki, N. Marinkovic, W. Xu, J. T. Muckerman, Y. Zhu and R. R. Adzic, *Energy Environ. Sci..*, 2013, **6**, 943 – 951.
8. W. Cui, N. Cheng, Q. Liu, C. Ge, A. M. Asiri and X. Sun, ACS Catal. 2014, **4**, 2658 – 2661.
9. D. H. Youn, S. Han, J. Y. Kim, J. Kim, H. Park, S. H. Choi and J. S. Lee, ACS Nano, 2014, **8**, 5164 – 5173.
10. L. F. Pan, Y. H. Li, S. Yang, P. F. Liu, M. Quan and H. G. Yang, *Chem. Commun.*, 2014, **50**, 13135 – 13137.
11. a) J. M. McEnaney, J. C. Crompton, J. F. Callejas, E. J. Popczun, A. J. Biacchi, N. S. Lewis and R. E. Schaak, *Chem. Mater.*, 2014, **26**, 4826−4831.; b) P. Xiao, M. A. Sk, L. Thia, X. Ge, R. J. Lim,J. Y. Wang, K. H. Lim and Xin Wang, *Energy Environ. Sci.*, 2014, **7**,

2624–2629.; c) X. Chen, D. Wang, Z. Wang, P. Zhou, Z. Wu and F. Jiang, *Chem. Commun*., 2014, **50**, 11683 –11685.
12. J. Xie, S. Li, X. Zhang, J. Zhang, R. Wang, H. Zhang, B. Pan and Y. Xie, *Chem. Sci.*, 2014, **5**, 4615 – 4620.
13. Y. Zheng, Y. Jiao, L. H. Li, T. Xing, Y. Chen, M. Jaroniec and S. Z. Qiao, ACS Nano, 2014, **8**, 5290 – 5296.
14. a) X. Zou, X. Huang, A. Goswami, R. Silva, B. R. Sathe, E. Mikmekova and T. Asefa, *Angew. Chem. Int. Ed.*, 2014, **53**, 4372 – 7376.; b) X. Zou, S. Gao, G. D. Li, Y. Liu, H. Chen, L. L. Feng, Y. Wang, M. Yang, D. Wang and S. Wang, *Nanoscale*, 2015, doi: 10.1039/C4NR04924A.
15. Y. Yin, R. M. Rioux, C. K. Erdonmez, S. Hughes, G. A. Somorjai and A. P. Alivisatos, *Science,* 2004, **304**, 711–714.
16. Q. Wang, Z. Lei, Y. Chen, Q. Ouyang, P. Gao, L. Qi, C. Zhu and J. Zhang, *J. Mater. Chem. A.,* 2013, 1, 11795–11801.
17. C.J. Ge, P. Jiang, W. Cui, Z.H. Pu, Z.C. Xing, A. M. Asiri, A. Y. Obaid and X. P. Sun, J. Tian, *Electrochim. Acta*,2014, **134**,182–186.
18 a) J. Bibsgaard, Z. Chen, B. N. Reinecke and T. F. Jaramillo, *Nat. Mater*. 2012, 11, 963 – 969.; b) J. A. Schaidle, A. C. Lausche and L. T. Thompson, *J. Catal.*, 2010, **272**, 235 – 245.
19. B. E., Conway and B. V. Tilak, *Electrochim. Acta*, 2002, **47**, 3571 – 3594.

Molybdenum carbide nanocrystals with a size less than 3 nm embedded in highly conductive N-doped carbon nanotubes exhibit superior activity for hydrogen evolution reaction, including small overpotential, large cathodic current density and high exchange current density.